The rotational spectrum and theoretical study of a dinuclear complex, MnRe(CO)10

The rotational spectrum and theoretical study of a dinuclear complex, MnRe(CO) 10

Chakree Tanjaroon, Kristen S. Keck, Stephen G. Kukolich, Michael H. Palmer, and Martyn F. Guest

Citation: The Journal of Chemical Physics **120**, 4715 (2004); doi: 10.1063/1.1637589
View online: http://dx.doi.org/10.1063/1.1637589
View Table of Contents: http://scitation.aip.org/content/aip/journal/jcp/120/10?ver=pdfcov
Published by the AIP Publishing

The rotational spectrum and theoretical study of a dinuclear complex, $MnRe(CO)_{10}$

Chakree Tanjaroon, Kristen S. Keck, and Stephen G. Kukolich[a)]
Department of Chemistry, University of Arizona, Tucson, Arizona 85721

Michael H. Palmer
School of Chemistry, University of Edinburgh, Scotland, United Kingdom

Martyn F. Guest
CLRC Daresbury Laboratory, Warrington, England, United Kingdom

(Received 30 September 2003; accepted 10 November 2003)

The first rotational spectrum of a dinuclear complex, $MnRe(CO)_{10}$, has been obtained using a high-resolution pulsed beam microwave spectrometer. Sixty-four hyperfine components of the $J=11\rightarrow J'=12$ and $J=12\rightarrow J'=13$ rotational transitions were measured for two rhenium isotopomers. The B values obtained from the experiment are $B=200.36871(18)$ MHz for the ^{187}Re isotopomer and $B=200.5561(10)$ MHz for the ^{185}Re isotopomer. The measured rotational constants are in reasonably good agreement with the B values calculated from the x-ray diffraction structural data, and from theoretical calculations. The gas-phase Mn–Re bond distance is approximately 2.99 Å, and the calculated value is only slightly longer. The experimental quadrupole coupling constant for the manganese atom is eQq_{aa} (^{55}Mn) $=-16.52(5)$ MHz, and the corresponding quadrupole coupling constants for the two rhenium isotopomers are eQq_{aa} (^{187}Re) $=370.4(4)$ MHz and eQq_{aa} (^{185}Re) $=390.9(6)$ MHz. The quadrupole coupling constants were also determined from a variety of theoretical calculations, with very large Gaussian orbital bases. The best estimates, at a nonrelativistic level, are eQq_{aa} (^{55}Mn) $=0.68$ MHz and eQq_{aa} (^{187}Re) $=327.6$ MHz with a 874 GTO basis set, but the results are very basis set dependent, especially the sign of the Mn quadrupole coupling. Very slight bending of angles $MnC_{eq}O_{eq}$ and $ReC_{eq}O_{eq}$ angles is found in the calculations. © *2004 American Institute of Physics.* [DOI: 10.1063/1.1637589]

I. INTRODUCTION

The study of transition metal carbonyl complexes and their derivatives is a very active and exciting area of chemical research. A recent review of the reactivity and synthesis of metal–metal bonded dinuclear complexes by Concolino and Eglin[1] provided a glimpse into this vast area of research. Over many decades, a number of useful and important compounds were discovered. Some of the most interesting ones were the metal–metal bonded derivatives of the dinuclear carbonyl complexes. For example, several chromium or molybdenum-based derivatives have been demonstrated to interfere with DNA replication by interacting with the base pairs. These biologically important derivatives are being developed as antitumor agents.[2–5] Other useful derivatives include the molybdenum or rhenium-based compounds, which are used as homogeneous catalysts and magnetic materials.[6–8] Other notable derivatives are the derivatives of dirhodium (II) acetates, known simply as Doyle catalysts.[9] Doyle catalysts are used effectively for the homogeneous asymmetric cyclopropanation, cyclopropenation, and intramolecular C–H insertion reactions.[10] All of these specialized compounds are derivatives of simple molecular building blocks, namely the metal–metal bonded carbonyl complexes. These building blocks are classified as either homo- or heterodinuclear carbonyl complexes [$M_2(CO)_n$, where M is a transition metal and n is integer]. In recent years, the heterodinuclear carbonyl complexes have received considerable research attention because of their chemical relevance in the synthesis of cluster complexes for catalysts.[11–13] One of the basic and useful building blocks for some of the heterodinuclear compounds is the $MnRe(CO)_{10}$ complex. Coville and Leins[14] have compiled a comprehensive review on the chemical and physical properties of the manganese rhenium decacarbonyl complex.

The $MnRe(CO)_{10}$ complex has served as a basic model for the study of heterodinuclear systems. The study of this complex has contributed much to our fundamental understanding about the electronic and structural properties, and the reactivity of metal–metal bonds.[15–21] $MnRe(CO)_{10}$ is a neutral coordination complex, stabilized by common strong π-acceptor CO ligands. Upon losing the carbonyl ligands due to heat or radiation, the fragmented dinuclear complex generally tends to become unstable and very reactive. The coordinatively unsaturated dinuclear fragments can undergo an intramolecular rearrangement to form a bridging complex via carbonyl ligand or interact with other suitable ligands. Brown and Zhang[22] have shown that the $MnRe(CO)_9$ fragment in hexane has one CO coordinated to the metals in a semibridging fashion. A bridging ligand can influence the chemical and physical properties of dinuclear compounds. For example, many bridged paddle wheel dichromium de-

a)Electronic mail: kukolich@u.arizona.edu

rivatives are known for their very short Cr–Cr bonds, and this has been ascribed to a quadruple bond between the two metals.[23,24] The strength and nature of metal–metal bonding can determine the molecular structure and influence the reactivity of dinuclear complexes.

The crystal structure of $MnRe(CO)_{10}$ had been reported earlier. The structure of $MnRe(CO)_{10}$ was first studied by Nesmeyanov and co-workers,[25] who reported the Mn–Re bond distance of 2.96 Å. In 1986, Rheingold, Meckstroth, and Ridge[26] redetermined the crystal structure, and reported an unexpectedly short Mn–Re bond distance of 2.909(1) Å for the $MnRe(CO)_{10}$ complex. Other measurements on similar Mn–Re dinuclear complexes[27–29] placed the value of the Mn–Re bond distance in the range of 2.817–2.96 Å. The exact molecular symmetry of $MnRe(CO)_{10}$ was not determined from these x-ray diffraction studies but was reported to be approximately D_{4d} symmetry.

We have now obtained the first pure rotational spectrum for the $MnRe(CO)_{10}$ complex. The complex exhibits a prolate symmetric-top rotational spectrum with hyperfine structure due to the Re and Mn nuclear quadrupole interactions. The complex has C_{4v} symmetry, with the principal C_4 symmetry axis along the axis (a axis) of the smallest moment of inertia, I_{aa}. We observed that the partially resolved hyperfine transitions are derived from two K stacks, with $K=0$ and 4. From consideration of the spin statistics for the $^{12}C^{16}O$ groups, which are exchanged by rotation about the C_4 principal axis (a axis), in a C_{4v}-symmetry molecule, the only transitions expected will involve the $K=4n$ states. Three molecular parameters were determined from least-squares fitting of the observed to the calculated rotational transitions. These molecular parameters are the B rotational constants for the ^{185}Re and ^{187}Re isotopomers, eQq_{aa} (^{185}Re) and eQq_{aa} (^{187}Re), the quadrupole coupling constants along the a axis for the ^{185}Re and ^{187}Re, and eQq_{aa} (^{55}Mn), the quadrupole coupling constant along the a axis for the ^{55}Mn. The measured rotational constants obtained from this study have allowed reasonably accurate estimates of the Mn–Re bond length.

In the present study, we also report a systematic theoretical study of the molecular equilibrium structure, electric quadrupole coupling strengths, and Mn–Re internuclear potential energy function for this complex. An important initial goal of the theoretical study was to give a sufficiently good prediction of the signs and relative magnitudes of the quadrupole coupling parameters to assist analysis of the experimental microwave data. Many recent density functional theory (DFT) calculations[30–33] have provided valuable insights into the electronic and molecular structures of homodinuclear complexes and their fragments. However, there are presently no reliable theoretical studies for heterodinuclear complexes and very few results for third-row mononuclear transition metal complexes. In this paper, we include theoretical calculations of quadrupole coupling strengths for $HMn(CO)_5$, $HRe(CO)_5$, and $MnRe(CO)_{10}$. Calculations on the mononuclear complexes were done to evaluate and test the methods. The calculations on the MnRe complex can assist in making assignments of measured lines, and the results can then be compared with final experimental results. In addition, comparison of the measured and calculated quadrupole-coupling constants for the $MnRe(CO)_{10}$ complex provide a sensitive probe for testing the accuracy of theoretical methods.

II. EXPERIMENT

The $MnRe(CO)_{10}$, complex was prepared following previously published synthetic procedures[34,35] with some modifications. All synthetic reactions were carried out under a nitrogen atmosphere. The $MnRe(CO)_{10}$ complex can be prepared by reacting either $Re(CO)_5Cl$ or $Re(CO)_5Br$ with $NaMn(CO)_5$ at room temperature. The following reagents were used to prepare the $MnRe(CO)_{10}$ complex: $Re(CO)_5Cl$ or $Re(CO)_5Br$ (Strem Chemicals:75-4000, 75-0150), and $NaMn(CO)_5$. Tetrahydrofuran (THF) was used as solvent and freshly distilled over sodium, in a nitrogen atmosphere, prior to use. $Re(CO)_5Br$ was prepared from $Re_2(CO)_{10}$ and liquid Br_2 using a well-published procedure.[36] The $NaMn(CO)_5$ salt was not available from commercial sources but was prepared using well-known synthetic procedures[34,35] with some modifications. The $NaMn(CO)_5$ salt was prepared by reacting $Mn_2(CO)_{10}$ with NaK(22% Na:78% K).[37] About 2.0 grams of $Mn_2(CO)_{10}$ was dissolved in 50.0 ml of THF and NaK was subsequently syringed into this solution in a 1:1 molar ratio. Right after the NaK was introduced to the yellow solution of $Mn_2(CO)_{10}$, the solution quickly turned bright red, indicating the reaction had started. After overnight stirring at room temperature, the $NaMn(CO)_5$ salt solution appeared as a dark orange colored solution. To the $NaMn(CO)_5$ salt solution, a 2:1 molar ratio solution of $Re(CO)_5Br$ or $Re(CO)_5Cl$ (in THF) was injected via a syringe. Following the injection of $Re(CO)_5Br$ or $Re(CO)_5Cl$ solution, the reaction flask was quickly purged with nitrogen and sealed tightly to prevent air from entering the flask. This reaction flask was then left to react for five days at room temperature. At the end of the five-day reaction period, THF was removed from the reaction flask under vacuum at room temperature. The resulting yellow solid residue was sublimed at 75 to 80 °C and 0.4 Torr. The air-sensitive $MnRe(CO)_{10}$ was a lemon yellow solid and often required a second sublimation to improve the purity.

Microwave data were collected using a Flygare–Balle type,[38] pulsed-beam Fourier transform microwave spectrometer operating in the 4–8 GHz range. This spectrometer was constructed in our laboratory,[39] following the general design given by Balle and Flygare,[38] and modified for these experiments as discussed below. The sample of $MnRe(CO)_{10}$ was placed into a glass sample cell, which is directly connected to the pulse valve. In order to produce sufficient vapor pressure from the solid sample, the glass cell and pulsed valve were heated to about 83 °C. This temperature was maintained throughout the experiment. The sample was pulsed into the microwave cavity, at a constant pulse rate of about 2 Hz, using neon as a carrier gas. The backing pressure of neon was maintained between 0.6–0.7 atm. The scanning was done between 4–5 GHz regions based on our ''best'' frequency predictions. Predictions of the frequencies were generated using coordinates produced from x-ray crystallographic data.[25,27] The frequency predictions obtained this

way were accurate within about $\pm 1.0\%$. Two rotational transitions with hyperfine splittings were measured in this experiment for each of the two rhenium isotopomers, $^{55}Mn^{185}Re(CO)_{10}$ and $^{55}Mn^{187}Re(CO)_{10}$. The measured transitions were relatively high J rotational transitions, $J=11 \rightarrow J'=12$ and $J=12 \rightarrow J'=13$. Many lower J transitions ($J<11$), which lie below 4 GHz, were not accessible using our current spectrometer. With the present configuration, our instrument operates in the 4–18 GHz frequency range.

The $MnRe(CO)_{10}$ complex has a large moment of inertia and fairly small permanent dipole moment. This made it quite difficult to observe the transitions. To help overcome this problem, a MITEQ low-noise amplifier (cooled with liquid N_2) was placed between the antenna in the Fabry–Perot cavity and the MITEQ balanced mixer to improve the spectrometer sensitivity. The MITEQ amplifiers used in our system are models JS2-020080-080-CR (2–8 GHz) and JS2-00160-150-CR (6–18 GHz). Even with the improved sensitivity, an average of 1000 beam pulses was required to obtain a signal-to-noise ratio better than 2/1. The spectral resolution with the Ne carrier gas is about 20.0 kHz.

III. THEORY

The theoretical studies were performed to determine the equilibrium structure for $MnRe(CO)_{10}$, and the electric field gradients (EFG) and nuclear quadrupole-coupling constants (NQCC), where neither the NQCC approximate magnitudes nor their signs were available from previous work. These new calculated values were useful for prediction of the experimental quadrupole splittings. Since the signs and magnitudes of the NQCC for both $HMn(CO)_5$ and $HRe(CO)_5$ complexes have been determined from previous microwave experiments,[40,41] the approach to the dinuclear compound was to study these two single metal carbonyl bonded complexes first. In this way, the basis sets necessary to give a good account of the Mn and Re quadrupole coupling would be determined in advance.

The first task was to find suitable basis sets for both Mn and Re which would be compatible with those of the (much smaller) H, C, and O atoms; the criteria for acceptability are that (a) the energy for the atoms should be close to best *ab initio* values. (b) All functions (GTOs) should make a significant contribution to the total density. (c) Since EFG calculations are sensitive to p orbitals in particular, a large level of uncontraction would be necessary to allow for core–valence polarization. Previous experience[42–45] with molecules having atoms having Z values up to that of iodine showed that the DZ (double zeta) and TZVP (triple zeta valence + polarization) bases of Huzinaga and Dunning[44,45] (for C,O, and H) are able to give good NQCC agreement with experiment for a variety of attached nuclei. A further feature, however, which emerged from these studies was that although bases contracted to double or triple zeta on the heavy atom gave good agreement with experimental structures, the quadrupole coupling at the halogen was often very low in magnitude. However, *when* the bases were effectively run *uncontracted*, then the structure was little changed, but the EFG now rose to values comparable with experimental ones. Finally, again because of the atomic size range, it became necessary to use uncontracted functions on the H, C, and O atoms as well. Hence, these approaches were applied to the present study, where GTO basis set sizes up to ~900 were used. The number of electrons makes more recent larger basis sets, such as the cc-pVTZ,[46] quite impracticable.

The Mn basis set was the Huzinaga (uncontracted $14s9p5d$) set[47] extended to $(14s10p7d)$. A series of calculations was performed with a single f function on Mn, with exponents in the range 1–10, but the atomic populations were always below 0.01e, and the effect on both the Mn–Re bond length and the EFG was found to be very small. Although effective core potential (ECP) bases such as LanL2DZ[48–52] are available for Re, the use of these is limited to determining an equilibrium structure (see below), since the core electrons contribute most of the EFG, and the lack of flexibility for the ''core'' parameters would not be expected to give accurate results. Thus, we determined an all-electron basis set for Re using previous studies,[53–56] with reported energies (E/a.u.) for $Re(^6S)$: −15 769.9 $(15s10p9d3f)$ (Ref. 52) −15 784.5 for both $(31s24p20d14f)$ (Ref. 54) and $(24s17p15d10f)$ (Ref. 55). The apparent near identity of the latter two studies, with rather different bases, suggested that reinvestigation would be significant. Thus, we reoptimized an Re basis, starting with a previous basis set for Sn, and making use of the reported relationship[42] between Gaussian exponents for two elements (nuclear charges Z_A, Z_B,), namely $\exp(A) \cong (Z_A/Z_B)^2 \times \exp(B)$. After further minor adjustments in the basis set, by scaling the exponents to achieve lower total energy, we obtained E−15 781.55 a.u. with $(21s15p11d6f)$. This energy is close to the best above, but achieved with a much more compact basis, and hence usable for large molecule calculations. These Re exponents were contracted $[s/p/d/f]$ to $[8,3,2,1^{11}/7^{12}/6,2,1^7/7,3]$, with similar treatment $[s/p/d]$ for Mn $[3,1^{11}/3,1^7/4,1^4]$; here, the superscript shows the number of single terms. In order to retain compatibility, the C, O $(11s6p1d)$ and H$(7s2p)$ functions were also largely uncontracted C, O $[5,1^6/3,1^4/1^2]$, and H$[1^7/1^2]$; these differ from the TZVP basis set by the addition of additional s,p,d functions of more diffuse character. Since the use of Cartesian GTOs leads to $6d$ and $10f$ functions, and the possibility of linear dependence through the implicit s- and p functions in these sets, respectively, most of the calculations required the use of the harmonic rather than Cartesian choice, with reduction in number of functions. This is exemplified in Table I as 417→392 (harmonic), etc. All the *ab initio* and DFT calculations were performed using the GAMESS-UK programming package.[57,58]

A. $HMn(CO)_5$ calculations

Some previous calculations of the $X\,^1A_1$ state with smaller bases and at the SCF and MP2 level have been reported.[59,60] Starting with $HMn(CO)_5$ and always assuming C_{4v} symmetry, Table I shows the results of several methods with several bases, and a comparison with the microwave spectral structure and the ED structure alone.[61] The former was based upon some calibration with neutron and electron diffraction (ED) data, and assumed linear MnCO groups. The most critical point is that although the larger bases give a

TABLE I. Comparison of the theoretical structures and electron distributions for $HMn(CO)_5$.

Basis	TZVP	Extended	Extended	Extended	Expt.	
Methodology	SCF	B3LYP	B3LYP	BP86	ED[58]	MW
NBasis	258	372→347	417→392	417→392		
Total E/a.u.	−1714.100	−1718.581	−1718.586	−1718.817		
H–Mn/Å	1.719	(1.645)	1.574	1.576	1.576	1.645(4)
$Mn-C_{ax}$	2.010	(1.822)	1.863	1.851	1.854	1.822
$C_{ax}-O_{ax}$	1.107	(1.143)	1.140	1.155	1.142	1.143
$Mn-C_{eq}$	2.037	(1.853)	1.863	1.848	1.856	1.853
$C_{eq}-O_{eq}$	1.107	(1.148)	1.137	1.152	1.142	1.148(2)
$Mn-C_{eq}O_{eq}$	174.4	(176.3)	177.2	177.4	169.9	176.3(15)
$H-Mn-C_{eq}$	83.5	(83.0)	83.2	83.2	85.5	83.0
$C_{ax}-Mn-C_{eq}$	96.5	(97.0)	96.8	96.8	94.5	97.0(4)
$cis-C_{eq}-Mn-C_{eq}$	89.3	(89.1)	89.2	89.2	89.6	89.1
$Trans-C_{eq}-Mn-C_{eq}$		(166.0)	166.5	166.3	169.7	166.0
EFG/a.u.	+0.6829	+0.6344	+0.7071	+0.6030		
^{55}Mn QCC/MHz[a]	−52.95	−49.19	−54.83	−46.75		−44.22

[a]The quadrupole moment for the ^{55}Mn isotope[68] is $+33fm^2$, giving a conversion factor of 77.54 MHz/a.u.

good account of many of the structural parameters, the H–Mn bond in particular is poorly determined in relation to this microwave structure, with the $Mn-C_{ax}$ bond also relatively poor. However, both these parameter values are very close to the ED study,[61] and some previous work.[62] The DZ and TZVP SCF calculations overestimate H–Mn, while the DFT (B3LYP and BP86) values are too short, with MP2 results even shorter. The atomic populations for the small bases seem quite unrealistic. Overall, the Becke–Perdew (BP86) study is marginally better than B3LYP, and gives the best structure and EFG, and of course, with the correct sign. The effect on the rotation constants, from these differences between the BP86 structure and the microwave structure, is fairly small [A,B are 903.7 MHz(calculated) to be compared with 908.0 MHz(from experiment)], in line with many equilibrium structure differences (0.5%) from experiment. The Mulliken atomic populations seem to have stabilized with the largest bases, but the effect of structure can be seen when the results of a B3LYP calculation at the experimental structure are compared with the equilibrium structure values. At r_e, the H atom is effectively neutral, with positive Mn being counterbalanced by CO polarization. Overall, the dipole moment is found to be very low (0.226D with the extended BP86 basis). In conclusion, while several factors remain unclear, particularly why the structure does not agree more closely with all aspects of the microwave one, the present calculations do provide some confidence that the ^{55}Mn quadrupole coupling constants are fairly stable with respect to both methodology and basis set (particularly in sign).

B. $HRe(CO)_5$ calculations

A C_{4v} equilibrium structure has been obtained by ECP methods, BP86 and B3LYP, similar to those for the manganese compound.[59] More recently, the ground and excited states were studied using the microwave structural parameters, with relativistic ECPs, containing a valence basis up to $(13s10p4d1f)$ for an effective $Z=15$.[63] In the present study, we initially used the LanL2DZ basis [with a 114 (harmonic) basis]; as can be seen, this gives a relatively good structure; as expected, the Re EFG is effectively zero, and quite different from experiment. However, when the extended basis set above, containing 434 (Cartesian) GTOs, was used *with the LanL2DZ structure*, the quadrupole coupling immediately returned with a value (−882 MHz) very close to experiment (−900 MHz). Thus, the large basis set is essential; this was then extended with the several bases using equilibrium structures from the SCF, BP86,[64,65] and B3LYP[66] Hamiltonians. All structures obtained are relatively close to that of the microwave study, including the "*cis*" bending of the carbonyl towards H rather than C_{ax}; the small bend in $\angle ReC_{eq}O_{eq}$ was also found in all calculations. In practice, all three studies gave NQCC values of the correct magnitude, with the B3LYP result being marginally better than the BP86 one, which was somewhat lower in magnitude. Table II shows the results of several methods of calculation, with various basis sets, and comparison with the structure from the present microwave work.

In summary, the present calculations do provide some confidence that both the ^{55}Mn and ^{187}Re quadrupole coupling constants are fairly stable with respect to both methodology and basis set (particularly in sign), while the larger bases give values within 10% of experiment. This is sufficient to make the study of the dinuclear species worthwhile. The effects of relativity are not included, but the pragmatic view that assistance with assignment of the microwave experiment would still be achieved.

C. $MnRe(CO)_{10}$ calculations

Initial structural optimization was performed with the LanL2MB and LanL2DZ bases, but the Mn–Re bond was large (3.67 and 3.429 Å, respectively) and, as with $HMn(CO)_5$, the EFG were negligible. Hence, the all-electron heavily uncontracted basis calculations for both Re and Mn were essential. The SCF procedure gave +117 MHz for the EFG at Re at the microwave structure, but the above studies suggested that DFT studies would be more profitable. The B3LYP method with the extended Mn and Re bases and TZVP (on C,O) basis sets gave a much shorter Mn–Re bond of 2.98 Å, and quadrupole couplings at Mn and Re of −4.53 and +521.95 MHz, respectively. Further extension of the

TABLE II. Comparison of the theoretical structures and electron distributions for $HRe(CO)_5$.

Basis set	DZ	Extended(1)	Extended	Extended	Microwave
Methodology	LanL2DZ	SCF	B3LYP	BP86	
NBasis	114	434→399	434→399	479→444	
Total E/a.u.	−642.490	−16341.038	−16348.733	−16349.942	
H–Re/Å	1.744	1.744	1.752	1.758	1.799(2)
$Re-C_{ax}$	2.008	2.008	2.088	2.073	2.000
$C_{ax}-O_{ax}$	1.146	1.146	1.139	1.150	1.130
$Re-C_{eq}$	2.023	2.023	2.066	2.053	2.000
$C_{eq}-O_{eq}$	1.140	1.140	1.137	1.150	1.1297
$Re-C_{eq}O_{eq}$	177.2	177.2	176.4	176.9	179.96
$H-Re-C_{eq}$	84.89	84.89	84.4	84.2	83.71
$C_{ax}-Re-C_{eq}$	95.1	95.1	95.6	95.8	96.275(5)
$cis-C_{eq}-Mn-C_{eq}$	89.6	89.6	89.5	89.4	89.31
$Trans-C_{eq}-Mn-C_{eq}$	169.8	169.8	168.9	168.4	167.43
Dipolemoment/D	0.6623	1.076	0.697	0.439	
^{187}Re EFG/a.u.	+0.0319	+1.8138	+1.8977	+1.7157	
$^{187}Re\chi_{zz}$ MHz	−15.53	−882.15	−923.00	−834.47	−900.13(3)

[a]The quadrupole moment for the ^{187}Re isotope (Ref. 68) is $+207fm^2$, giving a conversion factor of 486.37 MHz/a.u.

basis set with the BP86 methodology gave the Mn–Re bond as 3.22 Å, with quadrupole coupling +0.68(Mn) and +340.78 (Re) MHz, respectively. Crossovers between basis set size and methodology gave values shown in Table III, which were somewhat variable in Mn–Re bond length and in quadrupole coupling. If basis set effects are neglected, then Table III suggests that the Re quadrupole coupling decreases with bond length. However, basis sets *are* important, since a

TABLE III. Summary of theoretical structures and electron distributions for $MnRe(CO)_{10}$.

Basis set	Extended Mn+Re +TZVP(C, O)	Extended Mn+Re+C+ O	Extended Mn+Re+C+ O	Extended Mn+Re+C+ O	Extended Mn+Re+C+ O	Extended Re+C+O+ Mn (+f5.0)
Methodology	B3LYP	B3LYP	BP86	B3LYP	BP86	BP86
NBasis	638→588	784→724	784→724	874→814	874→814	882→819
Total E/a.u.	−18 070.502	−18 066.136	−18 067.589	−18 066.152	−18 067.595	−18 067.595
Dipolemoment /D	0.6839	1.4126	1.6470	1.4112	1.7336	1.5971
			Mn centered			
MnRe/Å	2.9752	3.2174	3.1922	3.2235	3.1400	3.1437
MnC_{ax}	1.8166	1.8161	1.8103	1.8231	1.8128	1.8100
$C_{ax}O_{ax}$	1.1441	1.1431	1.1580	1.1447	1.1585	1.1577
MnC_{eq}	1.8629	1.8667	1.8520	1.8642	1.8481	1.8522
$C_{eq}O_{eq}$	1.1414	1.1415	1.1558	1.1405	1.1561	1.1558
$MnC_{eq}O_{eq}$	174.4	176.20	175.96	176.59	175.34	175.51
$ReMnC_{eq}$	88.27	86.34	86.44	86.03	86.56	86.80
$C_{ax}MnC_{eq}$	91.73	95.27	93.56	93.97	93.44	93.20
$cis-C_{eq}MnC_{eq}$	89.95	89.77	89.78	89.73	89.79	89.82
$trans-C_{eq}MnC_{eq}$	176.55		172.87	172.06	173.12	173.59
$C_{ax}MnC_{eq}O_{eq}$	0.0	0.0	0.0	0.0	0.0	0.0
$ReMnC_{eq}O_{eq}$	180.0	180.0	180.0	180.0	180.0	180.0
EFG/a.u.	+0.0585	+0.0370	−0.0560	−0.0087	−0.0633	−0.0411
$^{55}Mn\chi_{zz}$ MHz	−4.5379	−2.8704	+4.3429	+0.6765	+4.9070	+3.1898
			Re centered			
ReC_{ax}	1.9381	1.9970	1.9835	1.9942	1.9705	1.9797
$C_{ax}O_{ax}$	1.1467	1.1417	1.1552	1.1412	1.1548	1.1551
ReC_{eq}	1.9927	2.0668	2.0554	2.0676	2.0589	2.0529
$C_{eq}O_{eq}$	1.1389	1.1365	1.1503	1.1366	1.1503	1.1503
$ReC_{eq}O_{eq}$	175.52	177.31	177.04	178.48	178.44	176.55
$MnReC_{eq}$	87.60	88.38	88.41	87.83	88.42	88.69
$C_{ax}ReC_{eq}$	92.40	91.62	91.59	92.17	91.58	91.31
$cis-C_{eq}ReC_{eq}$	89.90	89.95	89.96	89.92	89.96	89.97
$trans-C_{eq}ReC_{eq}$	175.20	176.76	176.81	175.66	176.83	177.38
$C_{ax}ReC_{eq}O_{eq}$	0.0	0.0	0.0	0.0	0.0	0.0
$MnReC_{eq}O_{eq}$	180.0	180.0	180.	180.0	180.0	180.0
EFG/a.u.	−1.0732	−0.6983	−1.0777	−0.6736	−0.8141	−0.9915
$^{187}Re\ \chi_{zz}$ MHz	+521.95	+339.63	+524.14	+327.60	+395.98	+482.24

TABLE IV. $MnRe(CO)_{10}$ B3LYP optimization with the 784 basis set using *Z*-matrix variables. Mn–Re bond lengths were at fixed values and all other variables are optimal (C_{4v} symmetry). The ^{187}Re and ^{55}Mn quadrupole coupling seems to be quadratic in bond length dependence (see Figs. 2 and 3).

	Mn–Re bond length/angstroms						
	2.60	2.80	3.00	3.20	3.40	3.60	3.80
OC_{ax} (Re)	1.143 2	1.142 2	1.141 8	1.141 7	1.141 7	1.141 8	1.141 9
$C_{ax}Re$	2.011 0	2.005 6	2.000 5	1.996 0	1.992 7	1.989 8	1.987 7
$C_{eq}Re$	2.072 1	2.069 8	2.068 9	2.068 6	2.068 8	2.069 5	2.070 3
$C_{ax}Mn$	1.820 2	1.818 5	1.818 0	1.818 1	1.817 9	1.818 0	1.817 8
$C_{eq}Mn$	1.865 6	1.864 2	1.864 7	1.866 1	1.867 9	1.870 0	1.872 0
OC_{ax} (Mn)	1.143 5	1.143 2	1.143 1	1.143 1	1.143 1	1.143 1	1.143 1
OC_{eq} (Mn)	1.142 3	1.142 1	1.141 9	1.141 6	1.141 4	1.141 2	1.141 0
OC_{eq} (Re)	1.137 2	1.136 8	1.136 6	1.136 6	1.136 5	1.136 6	1.136 7
	Bond angles/degrees						
$C_{ax}ReC_{eq}$	86.71	88.36	89.74	91.04	92.22	93.16	93.92
$ReMnC_{eq}$	90.76	89.13	87.68	86.47	85.44	84.61	84.00
$ReCO_{eq}$	172.23	173.80	175.13	176.35	177.46	178.41	179.19
$MnReC_{eq}$	93.29	91.64	90.26	88.96	87.78	86.84	86.08
$MnCO_{eq}$	173.43	174.37	175.25	176.03	176.87	177.64	178.25
$C_{ax}MnC_{eq}$	89.24	90.87	92.32	93.53	94.56	95.39	96.00
c-$C_{eq}MnC_{eq}$	89.99	89.99	89.91	89.78	89.64	89.49	89.37
t-$C_{eq}MnC_{eq}$	178.49	178.26	175.36	172.94	170.88	169.22	168.01
c-$C_{eq}ReC_{eq}$	89.81	89.95	90.00	89.98	89.91	89.83	89.73
t-$C_{eq}ReC_{eq}$	173.43	176.71	179.49	177.91	175.55	173.68	172.16
$MnReCO_{eq}$	180.0	180.0	180.0	180.0	180.0		
$C_{eq}ReC_{eq}O_{eq}$	86.72	88.36	89.74	91.04	92.22	93.16	93.91
$ReMnC_{eq}O_{eq}$	180.0	180.0	180.0	180.0	180.0		
$C_{eq}MnC_{eq}O_{eq}$	89.24	90.87	92.32	93.52	94.55	95.36	95.96
EFG Re/a.u.	+1.166 51	+0.434 51	−0.158 14	−0.618 28	−0.958 96	−1.196 08	−1.368 57
EFG Mn/a.u.	+0.553 50	+0.330 04	+0.163 80	+0.044 29	−0.035 83	−0.086 48	−0.117 43
χ Re/MHz	−567.354	−211.333	+76.913	+300.710	+466.407	+581.735	+665.633
χ Mn/MHz	−42.918	−25.592	−12.701	−3.434	+2.778	+6.705	+9.105
A/MHz	316.546	315.466	314.885	314.706	314.842	315.115	315.443
$B=C$/MHz	203.505	195.046	186.417	177.795	169.335	160.924	152.617

one-dimensional search using the 784 basis set showed that the variation in ^{187}Re QCC (Y/MHz) with Mn–Re bond length (X/Å) is closely fit by a quadratic function. The results of this calculation are shown in Table IV. The EFG values closely obey the following equations, where y = EFG/a.u., and the Mn–Re bond(x) is in angstrom units. The atomic quadrupole moment for ^{187}Re is 2.070(20) barn,[67,68] but the EFG are isotope independent within a specific atomic number,

$$\text{Re:}\quad y = 21.15(69) - 11.53(43)x + 1.48(7)x^2, \tag{1}$$

$$\text{Mn:}\quad y = 6.72(31) - 3.63(20)x + 0.48(3)x^2. \tag{2}$$

The internal ratios of the three terms ($y = A + B_1X + B_2X^2$) have $A(\text{Mn})/A(\text{Re}) = 0.318$, $B_1(\text{Mn})/B_1(\text{Re}) = 0.321$, and $B_2(\text{Mn})/B_2(\text{Re}) = 0.324$, and are clearly identical for the two isotopes, which seem to show very similar bonding at each of these atoms. The ratio is $2x(Q_{\text{Mn}}/Q_{\text{Re}})$ for these isotopes. Plots of the quadratic fit of Mn–Re bond length and EFG for the Mn and Re are given in Figs. 1 and 2. These results indicate that the dinuclear compound has a relatively weak bond, and hence is not easily treated by theoretical means. A plot of the Mn–Re bond energy for the $MnRe(CO)_{10}$ complex as a function of internuclear distance is shown in Fig. 3. The curve can be closely represented by a cubic equation in Mn–Re bond length (r) near the minimum, but over the $2.5 < r < 10$ Å range, a Morse potential provides a much better fit. This function has the form

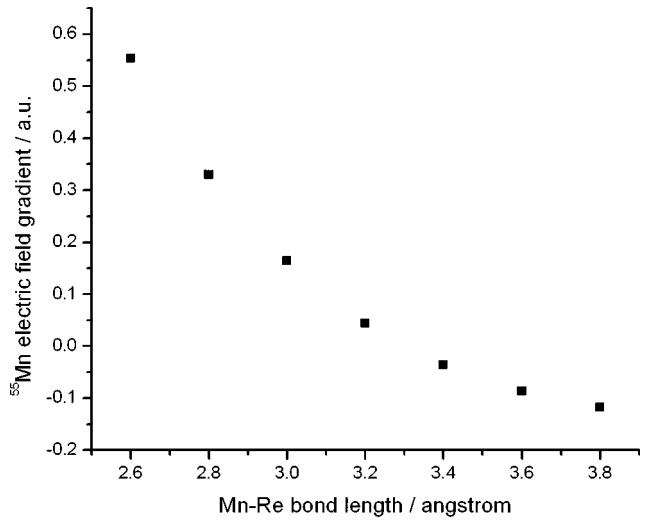

FIG. 1. Results of the quadratic fit of the ^{55}Mn electric field gradient (a.u.) vs Mn–Re bond length (Å). The EFG values closely obey the following equations, where y = EFG/a.u., and x = Mn–Re bond length: $y = 6.72(31) - 3.63(20)x + 0.48(3)x^2$.

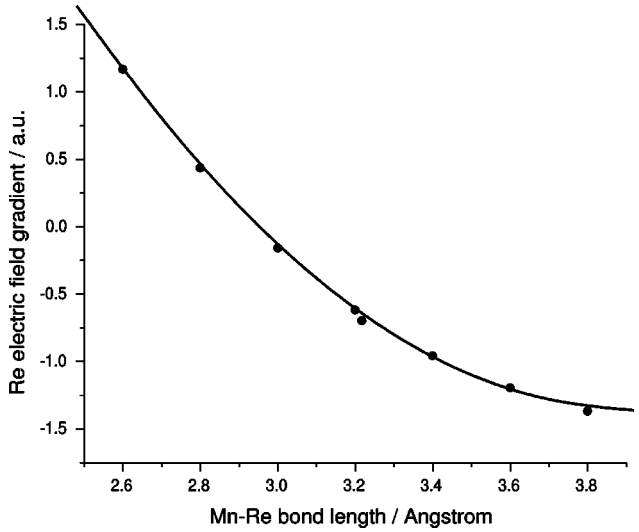

FIG. 2. The quadratic fit of the ^{187}Re electric field gradient (a.u.) vs Mn–Re bond length (Å). The EFG values closely obey the following equations, where y=EFG/a.u., and x=Mn–Re bond length: $y=21.15(69)-11.53(43)x+1.48(7)x^2$.

$$U(r)=U_0+D_e\{1-\exp[-\beta(r-r_e)]\}^2, \tag{3}$$

where $U_0=-0.1361(2)$ a.u., $D_e=0.0760(3)$ a.u., $\beta=0.884(4)$ Å^{-1}, and $r_e=3.210(3)$ Å. The minimum of this function is at 3.217 Å; this is very close to the experimental bond length. The dissociation energy is clearly low (2.07 eV), but to date no experimental value has been reported. However, although the Mn–Re bond length and quadrupole couplings vary with the calculation methodology and bases, the principal objective to determine the signs and approximate magnitudes of the couplings was achieved. Namely, the Mn coupling was small and probably negative, while the Re coupling was large and positive, and hence of opposite sign to that in $HRe(CO)_5$. The difficulty in extending the basis set or methodology further in order to attain more consistent results was impossible owing to limitations in the GAMESS-UK package in the use of (say) CASSCF optimization of the structure, while MP2 seemed unlikely to be useful.

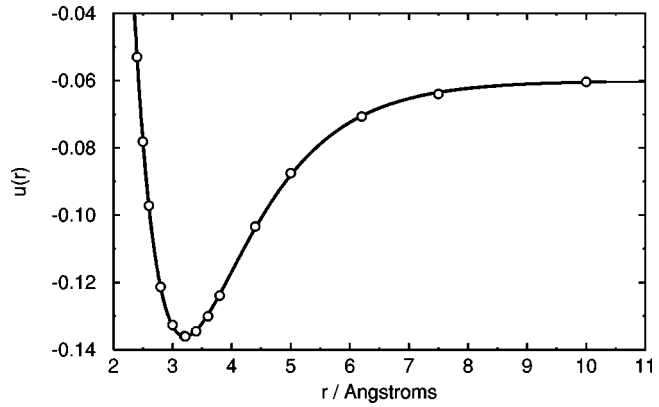

FIG. 3. A plot of the Mn–Re bond energy for the $MnRe(CO)_{10}$ complex as a function of internuclear distance. The solid is the Morse potential function: $U(r)=U_0+D_e\{1-\exp[-\beta(r-r_e)]\}^2$, where $U_0=-0.1361(1)$ a.u., $D_e=0.0760(3)$ a.u., $\beta=0.884(4)$ Å^{-1}, and $r_e=3.210(3)$ Å.

IV. FITTING AND RESULTS

Sixty-four observed rotational transitions for $MnRe(CO)_{10}$ were analyzed using spectral simulation and least-squares fitting methods. The transition frequencies for the simulation were calculated using a program originally from the University of Illinois (Flygare group—unpublished), and the fitting was done with the Pickett SPFIT,[69] fitting program. The observed hyperfine components of rotational transitions, $J=11\rightarrow J'=12$ and $J=12\rightarrow J'=13$, and deviations obtained from the least-squares fit analyses are listed in Tables V–VI. The measured rotational energies are assigned with the quantum numbers J, K, F and F, where F is the total angular momentum. To analyze and assign quantum numbers to the measured frequencies, all of the measured frequencies were plotted as a "stick plot" spectrum. This stick plot spectrum was then compared with a simulated theoretical spectrum. Three molecular parameters were used to simulate a theoretical spectrum. These parameters are $P_1=B$, rotational constant; $P_2=eQq_{aa}(Mn)$, the manganese quadrupole coupling constant; and $P_3=eQq_{aa}(Re)$, the rhenium quadrupole coupling constants. The B value of 202.5731 MHz for the main isotopomer was calculated from the x-ray diffraction structure.[27] Initial values for the rhenium and manganese quadrupole coupling constants were obtained from the DFT calculations, discussed in Sec. III. Using theoretical values of eQq_{aa} for Mn and Re, two sets of spectral simulations were determined for $J=11\rightarrow J'=12$ and for $J=12\rightarrow J'=13$ hyperfine transitions. The initial simulation using the values $P_1=340.8$ MHz, $P_2=0.68$ MHz, and $P_3=521.95$ MHz, gave a theoretical spectrum with hyperfine splitting patterns in reasonable agreement with the splitting pattern observed in the experimental stick plot spectrum. Further simulations with different P values were done to obtain a spectrum with "correct" hyperfine splitting patterns, by systematic adjustments to the initial P_1, P_2, and P_3 values, until good agreement between the theory and experiment was obtained. After careful comparison of the best simulation and experimental plots, we were able to tentatively assign proper quantum numbers to the experimental stick plot spectrum. The two sets of the assigned transitions clearly exhibited hyperfine splittings that derived mainly from two K components. The two observed K components were assigned to $K=0$ and $K=4$ states at this stage of analysis. Further spectral simulations were done using the Pickett SPCAT[69], prediction program and additional transitions were assigned including some for the $K=8$ state. This observation of only $K=4n$ transitions indicates that the molecular structure of $MnRe(CO)_{10}$ complex has a fourfold axis of symmetry and the complex most likely belongs to the point group C_{4v}. Figure 4 shows the molecular structure of $MnRe(CO)_{10}$ with the numbering of atoms indicated.

The accuracy of line assignments was confirmed using a least-squares fitting procedure. Three adjustable parameters were used in the Hamiltonian in order to fit the assigned transition frequencies for the two isotopomers (^{187}Re and ^{185}Re). These adjustable parameters are $P_1=B$, $P_2=eQq_{aa}(Mn)$, $P_3=eQq_{aa}(Re)$. The results for the measured and calculated (least-squares fit) transitions for the two isotopomers are shown in Tables V–VI. The standard deviations

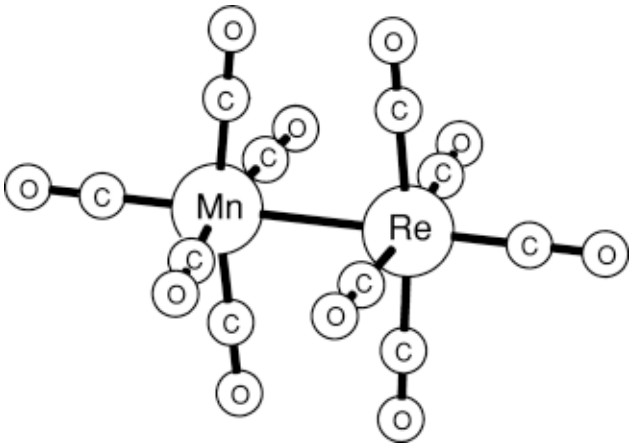

FIG. 4. The molecular structure of $MnRe(CO)_{10}$.

of these fits range from 6.0–7.0 kHz, indicating excellent fits. The resulting three molecular parameters obtained are shown in Table VII. From the spectral fitting results, the measured quadrupole coupling constant for the manganese is $eQq_{aa}(^{55}Mn) = -16.52(5)$ MHz. The measured quadrupole-coupling constant for $^{55}Mn^{187}Re(CO)_{10}$ is $eQq_{aa}(^{187}Re) = 370.42(38)$ MHz, and for $^{55}Mn^{185}Re(CO)_{10}$ is $eQq_{aa}(^{185}Re) = 390.91(56)$ MHz. The $Q(^{185}Re)/Q(^{187}Re)$ ratio obtained from this work is 1.055, which is in good agreement with earlier values [$Q(^{185}Re)/Q(^{187}Re) = 1.0567$, from Drouin, Cassak and Kukolich,[70] Table IV] and with the value from Gordy and Cook.[71]

The rotational constant obtained from the fits for the main isotopomer are $B = 200.3687(1)$ MHz. This microwave B value is about 1.0% smaller than the B value calculated from the x-ray structure,[27] which suggests that the gas phase structure of $MnRe(CO)_{10}$ is slightly larger than the solid phase structure (see Table VIII). Since limited isotopic data were obtained in the present study, the complete structure of $MnRe(CO)_{10}$ was not determined. However, some information about the Mn–Re bond length can be obtained from the measured rotational constants. The Mn–Re bond length can be estimated if we fix a number of the parameters to values from the crystal structure,[27] and then scale the Mn–Re bond length to fit the data. Thus, the C–O, Mn–C, and Re–C bond lengths were fixed: $r(Mn–C_{axial}) = 1.79$ Å, $r(Mn–C_{equatorial}) = 1.85$ Å, $r(MnC–O_{axial}) = 1.15$ Å, $r(MnC–O_{equatorial}) = 1.15$, $r(Re–C_{axial}) = 1.89$ Å, $r(Re–C_{equatorial}) = 1.98$ Å, $r(ReC–O_{axial}) = 1.18$ Å, $r(ReC–O_{equatorial}) = 1.13$. Similarly, the following angles were fixed (see Fig. 1): $C_2–Mn–C_4 = 169.1°$, $C_2–Mn–C_3 = 89.5°$, $Mn–C_1–O_1 = 180.0°$, $C_6–Re–C_9 = 174.02°$, $C_7–Re–C_8 = 89.8°$. The uncertainties, as estimated by Bau,[27] for bond lengths for Re–C or Mn–C and C–O are 0.03 and 0.04 Å, respectively. The uncertainty in bond angles is estimated at 1.0°. With the exception of the MnCO and ReCO bond angles and MnRe bond, these values are very similar to those calculated in the theoretical section above. Using the above fixed parameters, we obtained an eclipsed structure with C_{4v} symmetry. Finally, the Mn–Re bond length was scaled to yield a rotational constant which agreed with the experimental value. This led to a value for Mn–Re of 2.99 Å, slightly longer than the value previously reported by Ridge and co-workers[26] above.

TABLE V. Measured and calculated (best fit) frequencies for the $^{55}Mn^{185}Re(CO)_{10}$ dinuclear complex. Frequencies are given in MHz. Measurement errors are in parentheses. The standard deviation for the fit is 0.0067 MHz.

J	K	F	F	→	J'	K'	F'	F'	Observed	Observed-Calculated
11	4	12	12		12	4	12	12	4810.4353(27)	−0.0025
11	4	12	9		12	4	12	9	4810.5859(33)	−0.0012
11	8	10	12		12	8	11	13	4812.9990(25)	−0.0204
11	0	11	13		12	0	12	14	4813.8074(19)	0.0074
11	4	13	13		12	4	14	13	4813.8117(21)	0.0091
11	4	10	10		12	4	11	10	4813.8611(6)	−0.0036
11	0	11	11		12	0	12	11	4813.9933(40)	0.0016
11	0	10	9		12	0	11	10	4814.0228(31)	−0.0015
12	8	10	10		13	8	11	10	5207.6978(78)	−0.0052
12	8	10	11		13	8	11	12	5207.8244(54)	0.0066
12	4	10	11		13	4	11	11	5212.6100(82)	0.0059
12	0	13	15		13	0	14	15	5212.7544(17)	0.0011
12	4	15	13		13	4	16	14	5213.0109(155)	−0.0037
12	4	15	12		13	4	16	13	5213.0926(184)	0.0038
12	0	14	12		13	0	15	13	5214.0046(134)	0.0041
12	0	13	14		13	0	14	15	5214.3558(54)	0.0029
12	0	10	7		13	0	11	8	5214.7744(31)	−0.0034
12	4	11	12		13	4	12	13	5214.8541(41)	0.0108
12	4	11	13		13	4	12	14	5214.9145(42)	−0.0092
12	4	11	11		13	4	12	11	5214.9832(17)	−0.0061
12	4	13	14		13	4	14	14	5215.1167(35)	−0.0047
12	0	11	11		13	0	12	11	5215.3087(103)	0.0035
12	0	10	8		13	0	11	8	5216.2075(40)	0.0038

TABLE VI. Measured and calculated frequencies for the $^{55}Mn^{187}Re(CO)_{10}$ dinuclear complex. Frequencies are given in MHz. Measurement errors are in parentheses. The standard deviation for the fit is 0.0056 MHz.

J	K	F	F	→	J'	K'	F'	F'	Observed	Observed-Calculated
11	4	9	10		12	4	10	10	4806.6825(89)	−0.0063
11	0	11	13		12	0	12	13	4807.6992(74)	0.0003
11	4	9	8		12	4	10	9	4807.7254(29)	0.0105
11	0	10	12		12	0	11	12	4807.9142(20)	0.0050
11	4	9	7		12	4	10	7	4808.0691(96)	−0.0016
11	0	12	13		12	0	13	13	4808.1109(38)	0.0067
11	4	14	12		12	4	15	12	4808.2001(37)	−0.0013
11	8	10	8		12	8	11	9	4808.3563(22)	0.0028
11	0	14	13		12	0	15	14	4808.5672(57)	−0.0022
11	0	12	10		12	0	13	11	4808.7069(104)	0.0018
11	0	12	12		12	0	13	12	4808.9534(30)	−0.0044
11	0	10	11		12	0	11	11	4808.9650(27)	−0.0028
11	0	9	8		12	0	10	9	4809.1996(53)	0.0079
11	0	9	9		12	0	10	10	4809.2261(10)	0.0005
11	0	11	11		12	0	12	12	4809.2333(43)	−0.0035
11	0	9	11		12	0	10	12	4809.2542(37)	−0.0010
11	0	11	12		12	0	12	12	4809.2668(36)	0.0047
11	4	11	12		12	4	12	13	4809.2778(33)	−0.0004
11	4	11	10		12	4	12	11	4810.2242(33)	−0.0008
11	4	11	9		12	4	12	10	4810.2731(27)	−0.0042
11	4	12	12		12	4	13	12	4810.3660(4)	−0.0031
11	4	11	11		12	4	12	11	4810.3825(27)	−0.0042
11	4	12	11		12	4	13	11	4810.8356(34)	−0.0066
12	0	13	15		13	0	14	15	5207.8904(60)	−0.0021
12	0	14	13		13	0	15	14	5209.1555(25)	0.0022
12	0	14	14		13	0	15	15	5209.1657(34)	−0.0012
12	8	11	12		13	8	12	13	5209.2763(29)	−0.0112
12	4	14	15		13	4	15	15	5209.3143(30)	0.0005
12	0	10	11		13	0	11	11	5209.3252(38)	−0.0018
12	4	14	11		13	4	15	12	5209.8548(31)	−0.0088
12	0	12	10		13	0	13	11	5209.8966(27)	0.0024
12	4	11	11		13	4	12	11	5210.0981(24)	−0.0003
12	0	11	8		13	0	12	9	5210.1545(51)	−0.0004
12	0	10	10		13	0	11	10	5210.2117(50)	0.0143
12	4	13	12		13	4	14	12	5211.2985(22)	−0.0052
12	4	12	11		13	4	13	11	5211.3792(40)	0.0107
12	8	13	12		13	8	14	12	5214.1082(15)	0.0008
12	8	13	13		13	8	14	14	5214.1280(40)	0.0097
12	8	13	14		13	8	14	15	5214.2308(37)	0.0044
12	8	13	14		13	8	13	15	5214.2862(31)	−0.0109
12	8	12	14		13	8	12	14	5214.7278(14)	−0.0009

V. DISCUSSION

The rotational spectrum of $MnRe(CO)_{10}$ has been measured and analyzed to obtain the gas phase molecular parameters of the complex. The measured B value for $MnRe(CO)_{10}$ is 200.3687(2) MHz for the main isotopomer, which is about 1.0% smaller than the B value calculated from the x-ray structure,[27] and indicates a slightly larger structure in the gas phase. The more compact structure observed in the solid

TABLE VII. Molecular parameters obtained from the least-squares fit to the observed rotational transitions for $^{55}Mn^{185}Re(CO)_{10}$ and $^{55}Mn^{187}Re(CO)_{10}$. The values and error limits (2σ) are given in MHz. The standard deviations for the fits are in MHz.

Parameters	$^{55}Mn^{185}Re(CO)_{10}$	$^{55}Mn^{187}Re(CO)_{10}$
B	200.55602(13)	200.36871(8)
eQq_{aa}(Re)	390.91(56)	370.42(38)
eQq_{aa}(Mn)	−16.52(10)	−16.52(5)
σ(fit)	0.0067	0.0056
$Q(^{185}Re)/Q(^{187}Re)$	1.055	(This work)
$Q(^{185}Re)/Q(^{187}Re)$	1.05668(8)	(See Ref. 70)

TABLE VIII. Comparison of the experimental and theoretical molecular parameters for $Mn^{187}Re(CO)_{10}$. Rotational constants and eQq values are given in MHz. The r_{MnRe} bond length is given in angstrom. The standard errors 2σ are in MHz.

Parameters	$Mn^{187}Re(CO)_{10}$ This work	$Mn^{187}Re(CO)_{10}$ Theory	$MnRe(CO)_{10}$ X-ray[a]	$MnRe(CO)_{10}$ X-ray[b]
$eQq(^{55}Mn)$	−16.52(5)	0.68	-	-
$eQq(^{187}Re)$	370.42(38)	327.6	-	-
B	200.36871(8)	-	202.5731[c]	204.2304[c]
r_{MnRe}	2.99	3.22	2.96	2.909(1)

[a]References 7 and 16.
[b]Reference 8.
[c]Calculated from the geometry.

phase could be due to the presence of the crystal packing forces in the crystal. The Mn–Re bond length has been estimated in this work with the assumption that the gas phase metal–carbon and carbon–oxygen bond lengths and bond angles can be fixed to the values observed in the solid phase.[27] The Mn–Re bond length calculated with this scaling method is 2.99 Å, which appears to be in reasonably good agreement with the earlier solid-state value (2.96 Å) obtained by Nesmeyanov and co-workers[25] above. If we scale the Mn–Re bond length using the value (2.906 Å) reported by Ridge and co-workers[26] above, the rotational constant obtained from this scaling is about 204.0 MHz, and this is about 2% larger than the measured rotational constant. All these results suggest that the Mn–Re bond is slightly larger than the sum of the covalent radii (Mn:1.39, Re:1.53 Å, respectively).[72]

The quadrupole coupling constants along the symmetry axis (*a* axis) were obtained for the $MnRe(CO)_{10}$ complex. The results obtained for the manganese and rhenium quadrupole coupling constants in the calculations were rather variable, but consistent in pointing to a large positive value at Re, which contrasts with the $HRe(CO)_5$ molecule. Thus, the experimental $eQq_{aa}(^{187}Re)$ value [370.42(38) MHz] is close to the 874 basis set B3LYP and BP86 theoretical values of eQq_{aa} 327.6 and 339.6 MHz, respectively, and of course, of opposite sign to that in $HRe(CO)_5$. In contrast, the experimental quadrupole coupling constant for ^{55}Mn, eQq_{aa} $-16.51(7)$ MHz, is much larger in magnitude than the values predicted by the DFT calculations where the sign is not stable with respect to basis set and methodology. However, the difference in spectral and equilibrium bond lengths is clearly important at both centers, as discussed above, given the relationships of quadrupole coupling with bond length. The component of the quadrupole coupling tensor along the *a* axis for $MnRe(CO)_{10}$ is positive for rhenium and negative for manganese. The present Mn value is much reduced in magnitude when compared with the $HMn(CO)_5$ mononuclear compound.[40] The present experimental Re eQq is much smaller than the measured value for the $HRe(CO)_5$ mononuclear compound (-900 MHz), and of course reversed in sign. Both of these results indicate that for this dinuclear complex, the electronic charge distribution is more symmetrically distributed around the metal atoms than for the corresponding hydrides. There remains much work to be done experimentally and theoretically on this dinuclear complex. Many stronger rotational transitions (lower $J<10$) of this complex, which lie below 4 GHz, have yet to be measured. An apparatus is presently being constructed for lower frequency measurements. It is expected that the signals would be stronger and the hyperfine structure would be better resolved for the lower *J* transitions.

Calculations of electric field gradients and structures for third-row transition metal dinuclear complexes are difficult because of the equilibrium structure giving a metal–metal bond too long (weak) when compared with experiment. At present, the inability to perform large-scale multiconfiguration studies with a large active set of electrons is a real limitation, while MP2 also does not offer a good structure. For these elements, the large number of electrons and relativistic effects contribute to the difficulty in obtaining reliable results, since such effects are not well determined as yet. However, it is encouraging to note that the B3LYP and BP86 DFT Re quadrupole coupling strengths are relatively close to the measured value, and hence may prove useful in assisting other structural solutions.

ACKNOWLEDGMENTS

We gratefully acknowledge the National Science Foundation for providing financial support of this research. We thank Dr. Brian Drouin for help with the SPFIT fitting program. We thank the Edinburgh Parallel Computing Center for the provision of facilities on the Sun ''Sunfire 6800 SMP cluster'' and also Dr. P. J. Camp for the numerical fitting of the Morse curves.

[1] T. E. Concolino and J. L. Eglin, J. Cluster Sci. **8**(4), 461 (1997).
[2] P. Kopf-Maier and H. Kopf, Metal Compounds Cancer Therapy **109**, 46 (1994).
[3] F. O'Reilly, J. Kelly, and A. Kirsch-De Mesmaeker, Chem. Commun. (Cambridge) **9**, 1013 (1996).
[4] C. Liu, R. Yan, Y. Xu, S. Yu, Z. Lio, D. F. Li, and H.-B. F. Xu, in Proceedings of SPIE-The International Society for Optical Engineering (2001), 4414 (International Conference on Sensor Technology [ISTC(2001), 2001], pp. 43–46.
[5] S. P. Kaiwar, M. S. S. Raghavan, and C. P. Rao, J. Chem. Soc. Dalton Trans: Inorganic chemistry **10**, 1569 (1995).
[6] C. P. Casey, R. S. Carino, H. Sakaba, and R. K. Hayashi, Organometallics **15**, 2640 (1996).
[7] D. Bruce and D. O'Hare, *Inorganic Materials* (Wiley, New York, 1992).
[8] L. S. Hegedus, *Transition Metals in the Synthesis of Complex Organic Molecules* (University Science, 1994).
[9] M. P. Doyle and D. C. Forbes, Chem. Rev. **98**, 911 (1998).
[10] T. J. Colacot, Proceedings of Indian Acad. Sci. (Chem. Sci.). Vol. **112**, No. 3, pp. 197–207 (June 2000).
[11] W. L. Gladfelter and G. L. Geoffrey, Adv. Organomet. Chem. **18**, 207 (1980).
[12] D. A. Roberts and G. L. Geoffrey, in *Comprehensive Organometalic Chem.*, edited by G. Wilkinson, E. W. Abel, and F. G. A. Stone (Pergamon, Oxford, 1982), Vol. 6, p. 763.
[13] E. L. Meutterties, Science **196**, 839 (1997).
[14] N. J. Coville and A. E. Leins, J. Cluster Sci. **4**(3), 185 (1993).
[15] R. R. Andrea, A. Terpstra, D. J. Stufkens, and A. Oskram, Inorg. Chim. Acta **96**, L57 (1984).
[16] M. B. Hall, J. Am. Chem. Soc. **97**, 2057 (1975).
[17] J. Lewis and B. F. G. Johnson, Acc. Chem. Res. **8**, 245 (1968).
[18] G. A. Junk and H. J. Svec, J. Chem. Soc. A: Inorganic, Physical, Theoretical **12**, 2102 (1970).
[19] W. K. Meckstroth and D. P. Ridge, J. Am. Chem. Soc. **107**, 2281 (1985).
[20] G. Sbrignadello, G. Battistion, and G. Bor, Inorg. Chim. Acta **14**, 69 (1975).
[21] G. O. Evans, W. T. Wozniak, and R. K. Sheline, Inorg. Chem. **25**, 3608 (1970).
[22] T. L. Brown and S. Zhang, Inorg. Chem. **34**, 1164 (1995).
[23] F. A. Cotton, P. E. Fanwick, R. H. Niswander, and J. Sekutowski, J. Am. Chem. Soc. **100**, 4725 (1978).
[24] F. A. Cotton and T. Ren, J. Am. Chem. Soc. **114**, 2237 (1992).
[25] Y. T. Struchkov, K. N. Anisimov, O. P. Osipova, N. E. Kalobava, and A. N. Nesmeyanov, Dokl. Akad. Nauk SSSR, Ser. A **172**, 107 (1967).
[26] A. L. Rheingold, W. K. Meckstroth, and D. P. Ridge, Inorg. Chem. **25**, 3706 (1986).
[27] M. R. Churchill and R. Bau, Inorg. Chem. **6**, 2086 (1967).
[28] C. P. Casey, C. R. Cyr, R. L. Anderson, and D. F. Marten, J. Am. Chem. Soc. **97**, 3053 (1975).
[29] O. Orama, U. Schubert, F. R. Kreissl, and E. O. Fischer, Z. Naturforsch. B **35**, 82 (1980).
[30] H.-J. Freud, B. Dick, and G. Hohlneicher, Theor. Chim. Acta **57**, 185 (1980).
[31] T. A. Barckholtz and B. E. Bursten, J. Organomet. Chem. **596**, 212 (2000).
[32] E. Folga and T. Ziegler, J. Am. Chem. Soc. **115**, 5169 (1993).

[33] T. A. Barckholtz and B. E. Bursten, J. Am. Chem. Soc. **120**, 1926 (1998).
[34] N. Flitcroft, D. K. Huggins, and H. D. Kaesz, Inorg. Chem. **8**, 1123 (1964).
[35] S. P. Schmidt, F. Basolo, C. M. Jensen, and W. C. Trogler, J. Am. Chem. Soc. **108**, 1894 (1986).
[36] S. P. Schmidt, W. C. Trogler, and F. Basolo, Inorg. Synth. **28**, 160 (1990).
[37] J. E. Ellis and E. A. Flom, J. Organomet. Chem. **99**, 263 (1975).
[38] T. J. Balle and W. H. Flygare, Rev. Sci. Instrum. **52**, 33 (1981).
[39] R. E. Bumgarner, C. D. Cogley, and S. G. Kukolich, Chem. Phys. Lett. **122**, 535 (1985); R. E. Bumgarner and S. G. Kukolich, J. Chem. Phys. **86**, 1083 (1987).
[40] S. G. Kukolich and S. M. Sickafoose, Chem. Phys. Lett. **215**, 168 (1993).
[41] S. G. Kukolich and S. M. Sickafoose, J. Chem. Phys. **99**, 6465 (1993).
[42] M. H. Palmer, Z. Naturforsch., A: Phys. Sci. **53**, 370 (1998).
[43] M. H. Palmer, Z. Naturforsch., A: Phys. Sci. **53**, 383 (1998).
[44] T. H. Dunning, J. Chem. Phys. **53**, 2823 (1970).
[45] T. H. Dunning, J. Chem. Phys. **55**, 716 (1971).
[46] T. H. Dunning, J. Chem. Phys. **90**, 1007 (1989).
[47] S. Huzinaga, J. Chem. Phys. **66**, 4245 (1977).
[48] P. J. Hay and W. R. Wadt, J. Chem. Phys. **82**, 270 (1985).
[49] P. J. Hay and W. R. Wadt, J. Chem. Phys. **82**, 299 (1985).
[50] W. R. Wadt and P. J. Hay, J. Chem. Phys. **82**, 284 (1985).
[51] M. Dolg, H. Stoll, A. Savin, and H. Preuss, Theor. Chim. Acta **75**(3), 173 (1989).
[52] D. Andrae, U. Haussermann, M. Dolg, H. Stoll, and H. Preuss, Theor. Chim. Acta **78**, 247 (1991).
[53] J. Andzelm, M. Klobukowski, E. Radzio-Andzelm, Y. Saski, and H. Tatewaki, *Gaussian Basis Sets for Molecular Calculations*, edited by S. Huzinaga (Elsevier, Amsterdam, 1984).
[54] R. Poirier, R. Kari, and I. G. Csizmadia, *Handbook of Gaussian Basis Sets* (Elsevier Science, New York, 1985).
[55] E. Clementi, S. J. Chakravorty, G. Corongiu, and V. Sonnad, in *MOTECC-90 Modern Techniques in Computational Chemistry*, edited by E. Clementi (Escom, Leiden, 1990), pp. 47–140.
[56] S. Huzinaga and M. Klobukowski, J. Mol. Struct. **167**, 1 (1988).
[57] GAMESS-UK (V6.3): M. Dupuis, D. Spangler, and J. Wendoloski, NRCC Software Catalog, Vol. 1, Program No. QG01 (GAMESS), 1980.
[58] M. F. Guest, J. Kendrick, J. H. van Lenthe, K. Schoeffel, and P. Sherwood ''GAMESS-UK: Users Guide and Reference Manual,'' Version 5, Computing for Science (CFS) Ltd., Daresbury Laboratory, December 1994.
[59] V. Jonas and W. Thiel, J. Chem. Phys. **105**, 3636 (1996).
[60] M. R. J. Hachey and C. Daniel, Inorg. Chem. **37**, 1387 (1998).
[61] E. A. McNeill and F. R. Scholer, J. Am. Chem. Soc. **99**, 6243 (1977).
[62] D. Frigyes and G. Fogarasi, Organometallics **18**, 5245 (1999).
[63] J. Bossert, N. Ben Amor, A. Strich, and C. Daniel, Chem. Phys. Lett. **342**, 617 (2001).
[64] A. D. Becke, Phys. Rev. A **38**, 3098 (1988).
[65] J. P. Perdew, Phys. Rev. B **33**, 8822 (1986).
[66] A. D. Becke, J. Chem. Phys. **98**, 5648 (1993).
[67] P. Pyykkö, Mol. Phys. **99**, 1617 (2001).
[68] P. Raghaven, *Atomic and Nuclear Data Tables* (Academic, New York, 1989), **42**, 189.
[69] H. M. Pickett, J. Mol. Spectrosc. **148**, 371 (1997); see also: http://spec.jpl.nasa.gov/ftp/pub/calpgm
[70] B. J. Drouin, P. A. Cassak, and S. G. Kukolich, J. Chem. Phys. **108**, 8878 (1998).
[71] W. Gordy and R. L. Cook, *Microwave Molecular Spectra*, Vol. IX, Chemical Applications of Spectroscopy (Wiley, New York, 1968, 1970).
[72] F. A. Cotton and D. C. Richarson, Inorg. Chem. **5**, 1851 (1966).